

1 **The global groundwater resistome: core ARGs**
2 **and their dynamics - an *in silico* re-analysis of**
3 **publicly available groundwater metagenomes**

4 Ioannis D. Kampouris^{1,2,*}, Thomas U. Berendonk¹, Johan Bengtsson-
5 Palme^{3,4,5}, Uli Klümper^{1,*}

6

7 ¹ Institute of Hydrobiology, Technische Universität Dresden, 01217 Dresden, Germany

8 ² Arctic Research Centre, Department of Biology, Aarhus University, Aarhus, Denmark

9 ³ Division of Systems Biology, Department of Biology and Biological Engineering, Chalmers
10 University of Technology, SE-412 96 Gothenburg, Sweden

11 ⁴ Department of Infectious Diseases, Institute of Biomedicine, The Sahlgrenska Academy,
12 University of Gothenburg, Guldhedsgatan 10A, SE-413 46 Gothenburg, Sweden

13 ⁵ Centre for Antibiotic Resistance research (CARE) at University of Gothenburg, Gothenburg,
14 Sweden

15 * Corresponding authors

16 **Corresponding authors:**

17 Ioannis D. Kampouris (ORCID: 0000-0003-2093-5930) & Uli Klümper (ORCID: 0000-0002-

18 4169-6548)

19 Technische Universität Dresden

20 Institute of Hydrobiology

21 Zellescher Weg 40

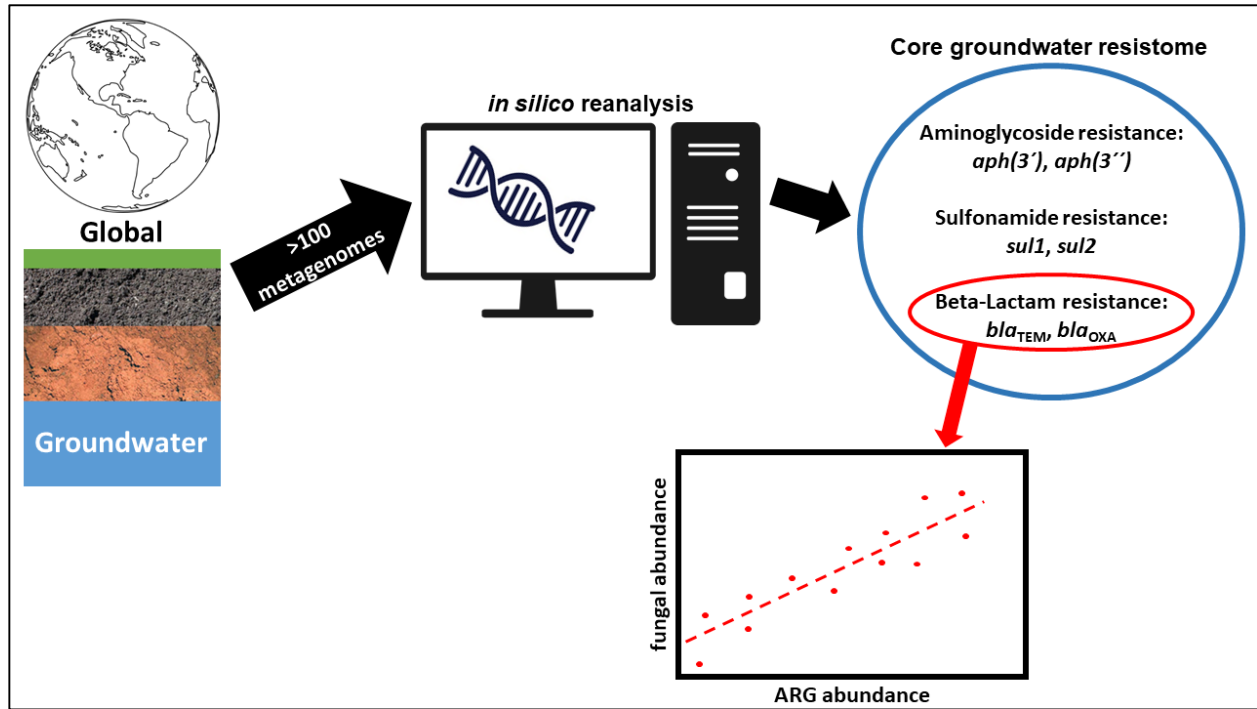
22 01062 Dresden

23 Germany

24 E-mail: ioannisds@yahoo.gr; uli.kluemper@tu-dresden.de

25 **Graphical abstract**

26



27

28

29 Abstract

30 Despite the importance of groundwater environments as drinking water resources, there is
31 currently no comprehensive picture of the global levels of antibiotic resistance genes in
32 groundwater. Moreover, the biotic and abiotic factors that might shape the groundwater
33 resistome remain to be explored on a global scale. Herein, we attempted to fill this knowledge
34 gap by *in silico* re-analysis of publicly available global groundwater metagenomes. We first
35 investigated the occurrence of antibiotic resistance genes (ARGs) to define the core
36 groundwater resistome. We further tested whether the ARG dissemination in the pristine
37 groundwater environments could be explained by natural ecological processes such as
38 competition between fungal and bacterial taxa. Six ARGs encoding resistance to
39 aminoglycosides (*aph(3')*, *aph(3'')*), sulfonamides (*sul1*, *sul2*), and β -lactams (*bla_{OXA}*, *bla_{TEM}*)
40 occurred in at least 50% of samples at high abundance, thereby constituting the core
41 groundwater resistome. ARG abundances differed significantly between countries and only
42 weakly correlated with bacterial community composition. While only limited effects of
43 anthropogenic impacts could be observed, ecological interactions played a significant role in
44 shaping the abundance patterns of at least a number of the core ARGs. Fungal abundance
45 positively correlated with *bla_{TEM}* and *bla_{OXA}* abundance, ARGs that confer resistance to β -
46 lactams, regularly produced by fungi. However, no direct correlation was determined for the
47 remainder of the core ARGs. Still, using co-occurrence network analysis we identified that the
48 fungal abundance acted as a hub-node that included *bla_{OXA}* and *bla_{TEM}*, but also indirectly
49 contributed to the abundance of aminoglycoside ARG *aph(3')*. Hence, interactions between
50 bacteria and fungi including potential antibiotic production can contribute to the dissemination of
51 ARGs in groundwater environments. Consequently, fungal/bacterial SSU ratio could serve as an
52 indicator for the abundance of certain ARGs in the pristine groundwater environments.

54 **Keywords**

55 Groundwater; Antimicrobial resistance; Antibiotic resistance; Fungi; Metagenomic re-analysis

56

57 **Highlights**

- 58 • Core GW resistome included *aph(3')*, *aph(3'')*, *sul1*, *sul2*, *bla_{OXa}* and *bla_{TEM}*
- 59 • Limited effects of anthropogenic impacts on GW resistome
- 60 • Fungal/bacterial abundance positively correlated with *bla_{TEM}* and *bla_{OXa}* abundance
- 61 • Fungal/bacterial abundance can serve as indicator for certain ARGs in groundwater

62

63 1. Introduction

64 The global rise in antimicrobial resistance (AMR) represents a major threat to future human
65 health ([Laxminarayan et al., 2013](#)). Tackling it requires a “One Health” approach that considers
66 AMR dynamics and proliferation between the human, veterinary and environmental spheres
67 ([Hernando-Amado et al., 2019](#)). Drinking water resources provide one of the immediate
68 connections between environmental and human microbiomes ([Vaz-Moreira et al., 2014](#)). Among
69 these, groundwater (GW) ecosystems constitute the most common freshwater and drinking
70 water resource in the majority of the world ([Szekeres et al., 2018](#); [Griebler and Avramov et al.,](#)
71 [2015](#); [Herrmann et al., 2019](#)). GW environments are characterized by high microbial diversity
72 and complexity ([Griebler and Lueders, 2009](#); [Flynn, et al., 2013](#); [Griebler and Avramov et al.,](#)
73 [2014](#)), with GW microbiota playing important roles in several biogeochemical cycles ([Flynn et](#)
74 [al., 2013](#); [Sonthiphand et al., 2019](#)). Due to the role of GW environments as a major drinking
75 water resource, understanding the occurrence of AMR in GW environments is highly relevant for
76 tackling AMR through a “One Health” approach ([Hernando-Amado et al., 2019](#)).

77 While several studies have focused on the importance of GW microbiota in biogeochemical
78 cycles ([Flynn et al., 2013](#); [Sonthiphand et al., 2019](#); [Retter et al., 2021](#)) or in their response to
79 pollution with toxic compounds ([Taş et al., 2018](#); [Sonthiphand et al., 2019](#)), only few have
80 looked into the occurrence dynamics of ARGs in GW using qPCR or metagenomic approaches
81 ([Szekeres et al., 2018](#); [Zhang et al., 2019](#); [Zaouri et al., 2020](#)). The potential anthropogenic
82 impact on AMR in GW was demonstrated for GW beneath a commercially operated wastewater
83 irrigated field ([Kampouris et al., 2022](#)). Here the abundance of specific antibiotic resistance
84 genes (ARGs) increased in accordance with the infiltration of the respective antibiotics from
85 wastewater into the GW. However, the majority of ARG abundance dynamics in more pristine
86 GW environments remains difficult to explain. Consequently, a global and comprehensive

87 picture of the natural ARG levels in GW and the non-anthropogenic factors that might shape the
88 GW resistome is needed.

89 Such global studies have been performed in terrestrial, non-anthropogenically impacted
90 environments, such as soil and surface marine waters, and generally linked ARG dissemination
91 partly to the competition between fungal and bacterial taxa (Bahram et al., 2018). Fungi
92 regularly thrive in soils, in close interaction with other biota (Bahram et al., 2018) and can
93 manipulate and shape the indigenous bacterial communities (Johnston et al., 2019). For
94 example, several fungal taxa produce β -lactam antibiotics (e.g. penicillin) (Aly et al., 2011).
95 Consequently, the specific complex fungi-bacteria interactions have been theorized as the
96 cause underlying the natural prevalence of β -lactam ARGs in the environment (e.g. occurrence
97 of *bla*_{TEM} and *bla*_{CTX-M} variants in relatively pristine soils) (Gatica et al., 2015). In GW
98 environments most of the detected fungi function as saprophytic organisms, enabling the
99 degradation of organic matter and performing organic carbon recycling (Nawaz et al., 2018).
100 However, how the presence of these fungi and the resulting fungal-bacteria interactions in the
101 humid, dark and pristine GW environments could affect the GW resistome has not yet been fully
102 explored.

103 Herein, we aimed to fill the knowledge gaps regarding which ARGs constitute the core global
104 GW resistome and if, similar to in pristine soils, interactions with fungi could provide an
105 explanatory variable in shaping it. To this end, we performed an *in silico* re-analysis of publicly
106 available global GW metagenomes retrieved from the NCBI sequencing read archive (SRA),
107 specifically investigating which genes constituted the core resistome and how they related to the
108 overall taxonomy of the GW communities.

109 **2. Methodology**

110 **2.1 Data collection of groundwater metagenomes**

111 Public metagenome datasets for samples from global GW environments were searched and
112 obtained from the NCBI sequencing read archive (SRA). The search queries included the terms
113 “groundwater”, “aquifer”, or “subsurface water”, for the matrices; and “shotgun sequencing” or
114 “wgs” for the sequencing method. The information from SRA was linked to publications and
115 locations, whenever available. Accession numbers and linked publications for all the retrieved
116 metagenomic datasets (100 metagenomes in total) are given in Table S1. An additional 30
117 identified candidate metagenomes from peer-reviewed studies were unfortunately not made
118 publicly available or did not pass the quality criteria presented in the next section and were
119 thereby excluded from the study.

120 **2.2 Annotation of antibiotic resistance gene profile and taxonomical composition**

121 For each metagenomic dataset general quality control and trimming were performed with the
122 tool cutadapt (v3.1, [Martin, 2011](#)), with the following command: cutadapt --cores=10 --cut 20 -q
123 10 --minimum-length 90 --max-n 0 --max-ee 0.1. The selection of a maximum expected error
124 (ee) of 0.1 allowed only high quality sequences to pass. Sequences with a length of less than 90
125 bp were filtered out, to ensure a sufficient read length for ARG annotation. ResFinder (Version
126 4), a database of mobile, acquired antibiotic resistance genes ([Bortolaia et al., 2020](#)) was
127 translated from nucleotide sequences into amino acid sequences using Biopython ([Cock et al.,](#)
128 [2009](#)). ARGs were annotated against the translated ResFinder database using the command
129 “blastx” in DIAMOND ([Buchfink et al., 2015](#)) with the following parameters: minimum identity
130 99%, minimum match length 30 amino acids. The parameters were chosen to be conservative
131 to reduce false positive hits. In case of paired-end sequencing, matches on the second paired
132 read were counted only if there was no match on the first read. The tool METAXA2 (version
133 2.2.3) ([Bengtsson-Palme et al., 2015](#)) was used for the identification of total small subunits of
134 ribosome (SSU), 16S rRNA for prokaryotes and 18S rRNA for eukaryotes, to determine
135 taxonomic composition, using the default settings. Screening for crAssphage sequences, an

136 indicator for anthropogenic fecal pollution, ([Karkman et al., 2019](#)) was performed with “ngless”
137 ([Coelho et al., 2019](#)), which utilizes a version of the BWA-MEM algorithm for alignment ([Li,](#)
138 [2013; Li and Durbin, 2010](#)).

139 To exclude any potential effects of differing sequencing depth on the estimated abundance of
140 ARGs, we performed a correlation of total ARG abundances with total bacterial counts. This
141 proved non-significant (Spearman rank correlation, $R=-0.17$, $p=0.1$, Fig. S1B), hence
142 sequencing depth can be excluded as a confounding factor.

143 **2.3 Data analyses and statistics**

144 Following ARG annotation and determination of the taxonomic composition, the results were
145 analyzed in R (v4.0, [R Core Team, 2019](#)). The total bacterial and fungal counts for each
146 metagenomic sample were calculated with the “tidyverse” packages (v1.0.4, [Wickham, 2019](#)).
147 The ARG, bacterial and fungal relative abundances were calculated similarly using the same
148 packages. The fungal 18S to bacterial 16S rRNA ratio was calculated using the “mutate”
149 function from the package “dplyr” (v.1.0.10, [Wickham et al., 2022](#)). The package “ggplot2”
150 (v.3.3, [Wickham, 2016](#)) was used for graphical representations.

151 Differences in the ARG composition based on Euclidean distance were visualized and
152 evaluated using the “vegan” package (v.2.5.6, [Oksanen et al., 2019](#)) by generation of NMDS
153 plots and statistical PERMANOVA tests. ARGs that were present with less than two reads in
154 less than four metagenomes from a single country were removed from the differential analysis
155 for ARGs. Countries with less than three available, high-quality metagenomes were excluded
156 from the location based analysis as well. All data was \log_{10} -transformed. Since the sequencing
157 depth of the retrieved metagenomes differed, for estimation of the differential gene abundances
158 and distance metrics we first calculated the limit of detection (LOD) of the different samples (Fig.
159 S1A). Then, zeros in abundance were replaced with an abundance of 10^{-8} gene/SSU, which

160 was one order of magnitude below the sample with lowest LOD (3×10^{-7}). The differences in
161 bacterial community composition were calculated similarly, with the sole exception that it was
162 based on the Bray-Curtis dissimilarity of bacterial taxa at the family level.

163 For comparing the differential abundance of every single ARG per location, the Kruskal-Wallis
164 test was performed with the use of the package “ggpubr” (v. 0.2.2, [Kassambara, 2019](#)). Mantel
165 and Procrustes tests between ARG profile (Euclidean distance) and bacterial community
166 composition (Family level, Bray-Curtis distance) were performed with the “vegan” package.

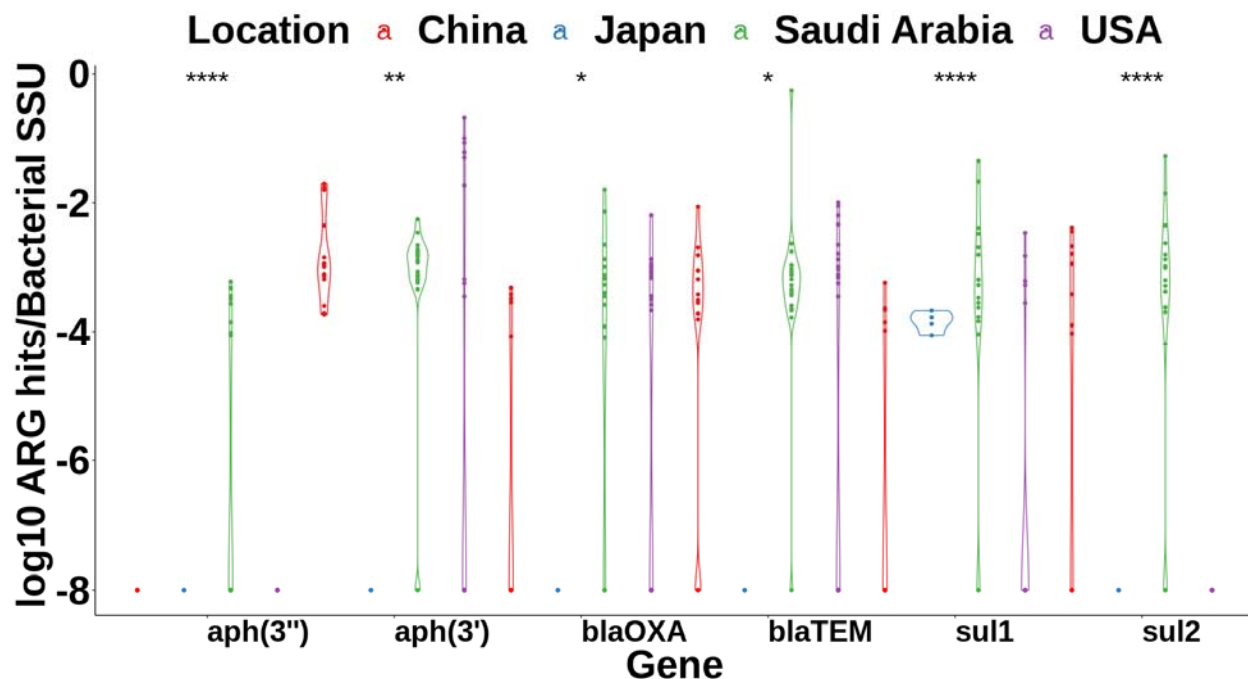
167 For correlation analyses, the data for different bacterial taxonomical groups, ARGs and
168 fungal/bacterial 16S rRNA ratio was \log_{10} transformed and Spearman correlations coefficients
169 were estimated with the package “ggpubr”. Samples with less than two positive hits for specific
170 taxonomical groups or ARGs were excluded from the correlation analysis. In addition, linear
171 mixed-effect models (package “lme4”, v1.1.3 [Bates et al., 2022](#)) were performed to account for
172 confounding variability in sampling, DNA extraction, etc., to subsequently verify the
173 hypothesized correlations. In these linear mixed-effect models, we used the original study of
174 each metagenome as random variable.

175 To reveal a) whether total fungal abundance correlates with changes in bacterial community
176 composition and b) whether these correlations can be linked to the fungal/ARG correlations, a
177 co-occurrence network was constructed using Spearman correlation and Benjamini-Hochberg
178 correction, with a threshold of $p < 0.05$. Samples without any positive hit were excluded to avoid
179 correlations due to zero inflated data. For inclusion in the co-occurrence network, a minimum
180 threshold was set: 25 samples with positive hits for each ARG or phylogenetic group. The co-
181 occurrence network was constructed with the packages “igraph” ([Csardi et al., 2005](#)) and
182 “ggraph” (v2, [Pedersen, 2022](#)).

183 3. Results and Discussion

184 3.1 The core groundwater resistome

185 In total 99 of the 100 screened metagenomes (Table S1) from diverse geographical locations,
186 including the US, Saudi Arabia, Japan and Germany, exceeded the high quality criteria (read
187 size <90 bp, expected error rate <0.1/read) for subsequent re-analysis. ARGs were successfully
188 detected in 87 of the 99 metagenomes. Overall, the common global GW resistome consisted of
189 24 ARGs which were detected in at least three metagenomes at abundances above 10^{-5} hits per
190 bacterial SSU (Fig. S2). These confer resistance to 13 antibiotic classes including
191 aminoglycosides, β -lactams, sulfonamides, and macrolides. Among these 24 ARGs, only the
192 sulfonamide ARGs *sul1* and *sul2*, the β -lactam ARGs *bla*_{OXA} and *bla*_{TEM} and the aminoglycoside
193 ARGs *aph*(3') and *aph*(3'') occurred in at least 50% of the metagenomes and throughout
194 displayed significantly higher relative abundances compared to the remaining ARGs (Kruskal-
195 Wallis test $p < 2.2 \times 10^{-16}$, Fig. S2). They hence constitute the core GW resistome (Fig. 1).



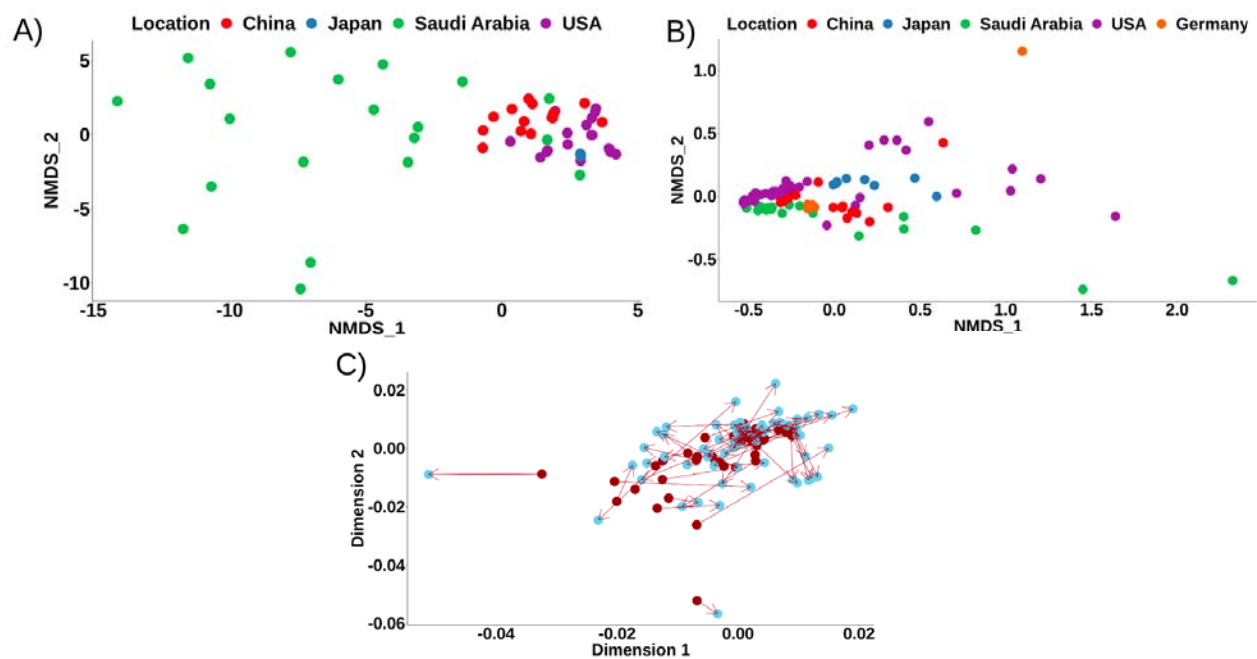
197 **Figure 1. Relative abundance of the ARGs that comprise the core resistome (occurred in at least 50% of the**
198 **metagenomes). Countries with less than three high-quality groundwater metagenomes in which ARGs were**
199 **detected, were excluded from this analysis. Significant differences were assessed with Kruskal-Wallis test**
200 **(* $p<0.05$, ** $p<0.01$, *** $p<0.001$, **** $p<0.0001$, $n=4-30$). Values of $\log_{10}\leq-8$ ARG hits/Bacterial SSU represent**
201 **samples with ARGs below the limit of detection, rather than actual values.**

202 Among the observed core ARGs, *bla*_{TEM} abundance was consistently higher, compared to other
203 β -lactam ARGs. Variants of *bla*_{TEM} have regularly been found to occur in high abundance in soil
204 microbiota, with no clear relation to anthropogenic influence (Gatica et al., 2013; Kampouris et
205 al., 2021; Wang et al., 2022). In previous studies, levels of *bla*_{TEM} were found to be similar
206 between wastewater and GW environments (Kampouris et al., 2021), while *bla*_{TEM} was the
207 dominant β -lactam ARG in GW environments, other β -lactam ARGs displayed up to two orders
208 of magnitude higher abundances than *bla*_{TEM} in wastewater (Kampouris et al., 2022). Similar
209 trends were observed when comparing pristine and agricultural soils in Germany (Kampouris et
210 al., 2021) and in China (Wang et al., 2022).

211 **3.2 Antibiotic resistance gene profiles diverge between different countries**

212 Resistome profiles based on the 24 detected common ARGs grouped significantly based on the
213 originating countries (Fig. 2A, PERMANOVA test, Euclidean Distance, $R^2=0.33$, $p=1\times 10^{-6}$, $n=4-$
214 30 ; sample number differed per-study). Abundances of most ARGs strongly depended on
215 location: for example, the highest abundance for most ARGs was detected in GW
216 metagenomes originating from Saudi Arabia (Fig. 1). This was especially true for those ARGs
217 that commonly occur in high abundance in wastewater microbiomes, such as *sul1* and *sul2*
218 (Caucci et al., 2016; Cacace et al., 2019) (Fig. 1, Kruskal Wallis, $p<0.001$, $n=4-30$). These two
219 genes confer resistance to sulfonamides, antibiotics of synthetic origin that have previously
220 been shown to accumulate in GW with parallel increase of sulfonamide ARGs, especially in
221 locations with extensive wastewater reuse for irrigation purposes (Avisar et al., 2009; Kampouris
222 et al., 2022). Indeed, rates of wastewater reuse in Middle Eastern countries such as Saudi

223 Arabia far exceed those in the other countries tested here (Jones et al., 2021; Liao et al., 2021).
224 Consequently, the direct infiltration of antibiotic resistant bacteria from wastewater irrigation, or
225 the infiltration of selective agents such as sulfonamide antibiotics could explain the increased
226 rates of ARGs in GWs of Saudi-Arabia. However, this hypothesis needs to be further tested,
227 since the herein analyzed metagenomes might have originated from sampling different depths
228 and types of GW environment (e.g. geyser or enclosed aquifer; Table S1), which could have
229 acted as a confounding variable on the differences in ARG profiles across the varying locations.



230

231 **Figure 2. A) NMDS grouping of ARG profiles of groundwater metagenomes by Euclidian distance based on**
232 **country of origin (PERMANOVA test, Euclidean Distance, $R^2=0.24$, $p=1 \times 10^{-6}$, $n=4-30$). ARGs that did not occur**
233 **in more than three metagenomes from at least one single country were excluded. Countries with less than**
234 **three high-quality groundwater metagenomes in which ARGs were detected, were also excluded from this**
235 **analysis. B) Bacterial community composition based clustering of groundwater metagenomes by Bray-Curtis**
236 **dissimilarity based on country of origin (PERMANOVA test, Bray-Curtis Distance, $R^2=0.33$, $p=1 \times 10^{-6}$, $n=6-41$).**
237 **C) Procrustes rotation plot between ARG profiles (Euclidean distance) and bacterial community composition**
238 **(Bray-Curtis distance). Procrustes rotation was used to rotate the dissimilarity matrix of the bacterial**
239 **community composition (β -diversity, Weighted Unifrac Distance) to maximum similarity with the target**

240 dissimilarity matrix of the ARG composition (Euclidean distance) by minimizing the sum of squared
241 differences. The Procrustes plot visualizes the association between bacterial community and ARG
242 composition. The length of the arrows visualizes the degree of match between the two ordinations following
243 Procrustes rotation (arrow-start: β -diversity, arrow-end: ARG composition). Mantel test, Spearman
244 correlation $\rho=0.25$, $p=0.001$, Procrustes test $\rho=0.62$, $n=69$.

245 To determine if such a potential direct effect of infiltration of fecal microorganisms to these GW
246 environments exists, we quantified the abundance of crAssphage in the samples, which has
247 been suggested as an indicator of pollution with fecal anthropogenic microorganisms (Karkman
248 et al., 2019). Consequently, crAssphage presence would indicate that wastewater derived
249 organisms were the main driving force underlying increased ARG abundance in these GW
250 environments. However, no crAssphage reads were detected in any of the studied
251 metagenomes, indicating that the infiltration of fecal organisms can be excluded as an
252 explanatory variable for the increased levels of *sul1* and *sul2*. Still, the infiltration of selective
253 agents independent of fecal organisms remains an option that has previously been observed for
254 certain GW environments (Kampouris et al., 2022). However, this could not be tested in this
255 study due to the lack of associated metadata on concentrations of antibiotics.

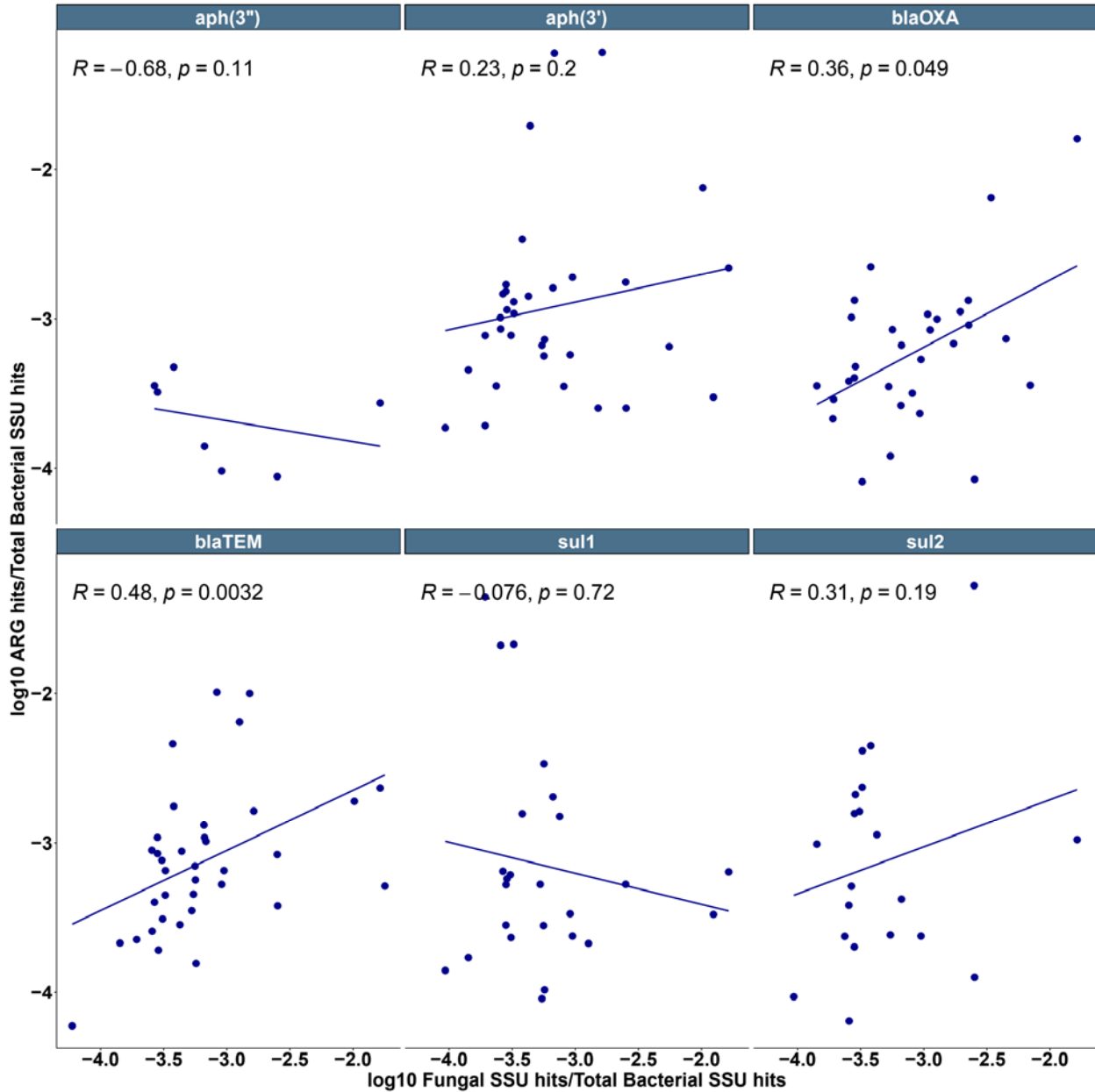
256 Similar to ARG profiles, the bacterial community compositions clustered by countries (Fig. 2B,
257 PERMANOVA test, Bray-Curtis distance, $R^2=0.24$, $p=10^{-6}$, $n=6-41$; sample number differed per-
258 study). Still, bacterial community composition dissimilarity provided only a minor explanation for
259 ARG compositional dissimilarities as only a weak significant correlation was found (Mantel test,
260 Spearman correlation $\rho=0.25$, $p=0.001$, Procrustes test, $\rho = 0.62$, $n=69$, Fig. 2C).

261 **3.3 Correlation of fungal and antibiotic resistance gene abundances in groundwater** 262 **metagenomes**

263 Aside from bacterial community composition, we aimed at further exploring the underlying
264 drivers of resistome diversity and abundance in the GW microbiota by evaluating if ecological

265 interactions with natural producers of antibiotics such as fungi and *Actinobacteria* could play a
266 role in ARG dissemination (Bahram et al., 2018). Fungal activity has indeed been hypothesized
267 to contribute to ARG dissemination and maintenance in environments with low levels of
268 anthropogenic pollution with bacteria or selective agents (Bahram et al., 2018). We hence
269 evaluated the correlation of the six core GW ARGs with fungal relative abundance
270 (fungal/bacterial SSUs in the metagenomes). A clear correlation between fungal per bacterial
271 abundance and bla_{TEM} abundance (Spearman $\rho=0.48$, $p=0.0039$, Fig. 3) and a weak but
272 significant correlation for bla_{OXA} abundance (Spearman $\rho=0.36$, $p=0.049$, Fig. 3) were
273 observed. No correlation was detected for the remaining core GW ARGs ($sul1$, $sul2$, $aph(3')$,
274 $aph(3'')$, $p>0.05$). Consequently, fungal abundance correlated mainly with the levels of bla_{TEM}
275 and bla_{OXA} , which confer resistance to β -lactam antibiotics, commonly produced by several
276 fungal species as secondary metabolites (Nesme and Simonet, 2015). The observed
277 correlations for bla_{TEM} and bla_{OXA} were further verified using a linear mixed model. Here, the
278 original study that the metagenomes were derived from was set as a random effect variable to
279 counter potential study based biases (ARG Rel. Abundance \sim Fungal Rel. Abundance +
280 1|Original_Study) ($p=0.0152$). When reducing study based biases with the linear mixed model
281 the previously barely significant correlation for bla_{OXA} ($p=0.049$) clearly increased in significance
282 ($p=0.008$).

283 We further examined the correlation of ARG abundance with *Actinobacteria*, known as the
284 major group of bacterial antibiotic producers (Miao et al., 2010). *Actinobacteria* and bla_{TEM}
285 abundance weakly correlated initially ($p=0.047$, Fig. S3), but this could not be confirmed using
286 the linear mixed model ($p>0.05$, ARG Rel. Abundance \sim *Actinobacteria* Rel. Abundance +
287 1|Original_Study). None of the remaining core-resistome ARGs significantly correlated with
288 *Actinobacteria* abundance ($p>0.05$, Fig. S3).



289

290 **Figure 3. Linear regression and correlation of the relative abundance of individual core groundwater ARGs to**
291 **ribosomal fungal/bacterial small subunit (SSU) ratio (Spearman rank-correlation). Samples without fungal or**
292 **ARG counts were excluded.**

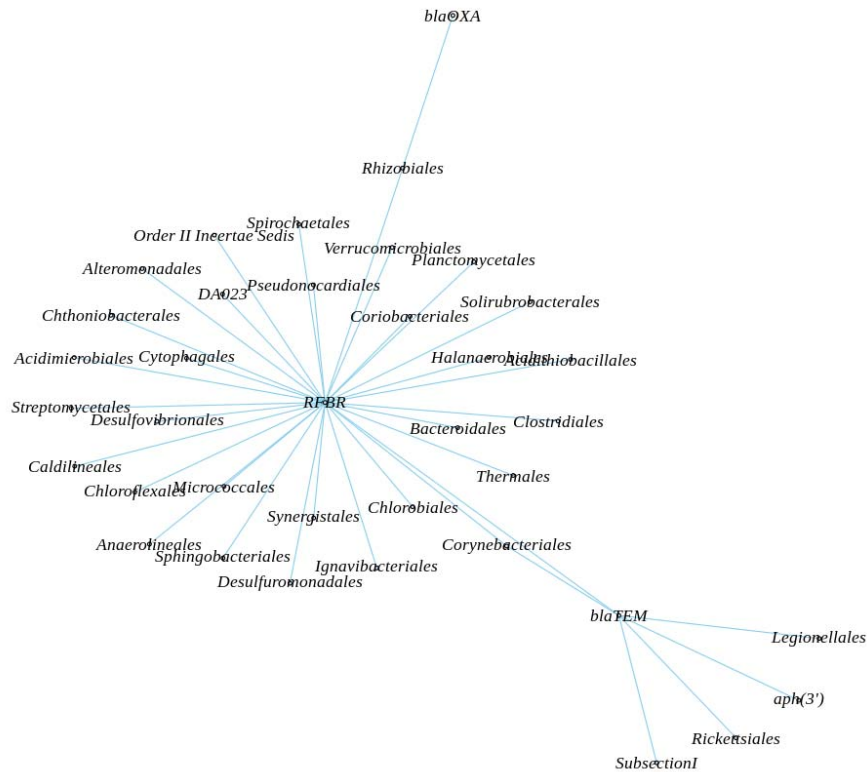
293 **3.4 Fungal abundance might serve as an indicator for ARG abundance in groundwater** 294 **environments**

295 To further explore if fungal relative abundance can explain ARG GW dynamics, co-occurrence
296 network analysis (Spearman correlation, $p < 0.05$, Benjamini-Hochberg correction) with bacterial

297 community composition (lowest taxonomical level: Order), fungi/bacteria SSU ratio and ARG
298 abundances was performed. Of all 24 ARGs tested only three of the core GW ARGs *bla*_{TEM},
299 *bla*_{OXA} and *aph*(3') were included as a part of the correlation network (Fig. S4). As two of these
300 were already previously associated with positive correlations with fungal abundance we
301 extracted all correlations from the network which either one of the ARGs or the fungal/bacterial
302 SSU ratio were a part of (Fig. 4). The three ARGs as well as the fungal/bacterial SSU ratio were
303 part of one interconnected node hub. More specifically, all ARGs showed a direct or indirect
304 connection (one common link) to the fungal/bacterial SSU ratio. Furthermore, all extracted
305 correlations directly or indirectly connecting ARGs with fungal/bacterial SSU ratio were positive
306 (Fig. 4). Specifically, *bla*_{TEM} was directly positively correlated with fungal/bacterial SSU ratio and
307 further indirectly connected through the bacterial order of *Corynebacteriales*, supporting the
308 previously detected strong correlation of this ARG. Moreover, the relative abundance of *bla*_{TEM}
309 was the only explanatory factor connected to the aminoglycoside ARG *aph*(3') (Fig. 4), which
310 supports the previously indicated weaker positive correlation with fungal relative abundance.
311 Meanwhile, *bla*_{OXA} was exclusively connected to the bacterial order of *Rhizobiales*, which was in
312 turn providing the indirect link through positive correlation with the fungal/bacterial SSU ratio
313 based on Spearman correlations.

314 In addition to the ARGs, fungal abundance was positively correlated with a number of individual
315 bacterial taxa, however not a single antagonistic interaction was observed (Fig. 4). These
316 observed positive correlations indicate potential mutualistic interactions. Selection for specific
317 bacterial taxa was driven by their ability to co-exist with fungi, despite the potential production of
318 secondary metabolites by fungi with negative effects on bacterial growth. Since β -lactam ARGs
319 confer resistance to β -lactam antibiotic, which are commonly produced antibiotics by fungi (Aly
320 et al., 2011), we hypothesize that these ARGs could potentially have enabled the co-existence

321 of several of these bacterial taxa with fungi, hence promoting their co-occurrence as individual,
322 interconnected nodes within the correlation network centering around fungal abundance.



323

324 **Figure 4. Extract of correlations including either the ribosomal fungal/bacterial SSU ratio (RFBR) or any of**
325 **the detected ARGs from the full co-occurrence network (Fig. S3). Only significant correlations based on**
326 **Spearman Correlation with Benjamini-Hochberg correction for multiple testing ($p < 0.05$) are shown. All**
327 **extracted correlations within this network were significantly positive.**

328 In summary, ARGs were regularly only directly connected to a minor proportion of taxa but
329 rather directly or indirectly connected to fungal abundance with positive correlations.
330 Consequently, fungal abundance might serve as a better indicator for the abundance of certain
331 ARGs in GW microbiomes than the bacterial community composition itself.

332 **3.5 Summary of results**

333 In the present *in silico* study we identified the common and core ARGs that make up the global
334 GW resistome and elucidated potential drivers underlying their abundance patterns. The
335 common GW ARGs conferred resistance to 13 antibiotic classes, while the core resistome was
336 made up of six ARGs conferring resistance to sulfonamides, β -lactams and aminoglycosides.
337 Local patterns regarding the intensity of anthropogenic factors were identified as a driving force
338 behind the distribution of ARGs conferring resistance to the synthetic antibiotic class of
339 sulfonamides. However, for β -lactams - natural, fungal-derived antibiotics (Nesme and Simonet,
340 2015) - the relative abundance of these fungi provided a main explanatory variable. A previous
341 investigation on global soil microbiota supports such a correlation of fungi with total ARGs
342 (Bahram et al., 2018). While across soils co-selective effects for a number of antibiotic classes
343 could be detected, in GW metagenomes only the β -lactam ARGs bla_{TEM} and bla_{OXA} were directly
344 correlated with fungal abundance. In addition, fungal abundance served as indirect indication for
345 the aminoglycoside ARG $aph(3')$, which belonged to the core GW resistome and indirectly
346 correlated with fungal abundance through co-occurrence network analysis.

347 **4. Conclusion**

348 Overall we show that the re-analysis of publicly available data is a valuable tool for testing
349 hypotheses currently present in the microbial ecology spectrum and elucidating potential global
350 relationships between different microbial groups in GW environments. Specifically, we
351 demonstrated that in the pristine GW environments, the global resistome is dominated by a
352 small number of ARGs and that their abundance profiles, where mostly influenced by local
353 conditions, while they can be partially shaped by microbe-microbe interactions. By using these
354 *in silico* approaches we can pinpoint and identify potential microbe-microbe interactions for
355 further verification in controlled laboratory experiments. In addition, we demonstrated that the
356 bacterial/fungal SSU ratio could act as a direct and indirect indicator for the abundance of

357 specific ARGs in GW environments. We expect that with the increase of publicly available data,
358 such *in silico* meta-analyses will be able to further identify ecological interactions in
359 understudied environments in the future.

360 **5. Conflict of interest**

361 The authors declare no conflict of interest.

362 **6. Acknowledgements**

363 We deeply thank the researchers that uploaded and provided their sequencing data in the NCBI
364 SRA databases, as without their contribution this study would have been impossible.

365 **7. Funding**

366 This work was supported by the JPI AMR - EMBARK and the ANTIVERSA project funded by
367 the Bundesministerium für Bildung, und Forschung under grant numbers & F01KI1909A &
368 01LC1904A, and the European Union's Horizon 2020 research and innovation program under
369 the PRIMA program supported by the European Union under grant agreement No 1822. JBP
370 acknowledges funding from the Swedish Research Council (VR; grant 2019-00299) under the
371 frame of JPI AMR (EMBARK; JPIAMR2019-109) and the Data-Driven Life Science (DDLs)
372 program supported by the Knut and Alice Wallenberg Foundation (KAW 2020.0239).
373 Responsibility for the information and views expressed therein lies entirely with the authors.

374 **8. Data availability**

375 Data and the R and shell scripts for the workflow of analysis have been uploaded in
376 https://github.com/JonKampouris/GW_Resistome.

377

9. References

378

1) Aly, A.H., Debbab, A., Proksch, P., 2011. Fungal endophytes: Unique plant inhabitants

379

with great promises. *Appl. Microbiol. Biotechnol.* 90, 1829–1845.

380

<https://doi.org/10.1007/s00253-011-3270-y>

381

2) Alygizakis, N.A., Urik, J., Beretsou, V.G., Kampouris, I., Galani, A., Oswaldova, M.,

382

Berendonk, T., Oswald, P., Thomaidis, N.S., Slobodnik, J., Vrana, B., Fatta-Kassinou,

383

D., 2020. Evaluation of chemical and biological contaminants of emerging concern in

384

treated wastewater intended for agricultural reuse. *Environ. Int.* 138, 105597.

385

<https://doi.org/10.1016/j.envint.2020.105597>

386

3) Avisar, D., Lester, Y., Ronen, D., 2009. Sulfamethoxazole contamination of a deep

387

phreatic aquifer. *Sci. Total Environ.* 407, 4278–4282.

388

<https://doi.org/10.1016/j.scitotenv.2009.03.032>

389

4) Bahram, M., Hildebrand, F., Forslund, S.K., Anderson, J.L., Soudzilovskaia, N.A.,

390

Bodegom, P.M., Bengtsson-Palme, J., Anslan, S., Coelho, L.P., Harend, H., Huerta-

391

Cepas, J., Medema, M.H., Maltz, M.R., Mundra, S., Olsson, P.A., Pent, M., Pölme, S.,

392

Sunagawa, S., Ryberg, M., Tedersoo, L., Bork, P., 2018. Structure and function of the

393

global topsoil microbiome. *Nature* 560, 233–237. <https://doi.org/10.1038/s41586-018->

394

0386-6

395

5) Bengtsson-Palme, J., Larsson, D.G.J., 2016. Concentrations of antibiotics predicted to

396

select for resistant bacteria: Proposed limits for environmental regulation. *Environ. Int.*

397

86, 140–149. <https://doi.org/10.1016/j.envint.2015.10.015>

398

6) Bortolaia, V., Kaas, R.S., Ruppe, E., Roberts, M.C., Schwarz, S., Cattoir, V., Philippon,

399

A., Allesoe, R.L., Rebelo, A.R., Florensa, A.F., Fagelhauer, L., Chakraborty, T.,

- 400 Neumann, B., Werner, G., Bender, J.K., Stingl, K., Nguyen, M., Coppens, J., Xavier,
401 B.B., Malhotra-Kumar, S., Westh, H., Pinholt, M., Anjum, M.F., Duggett, N.A., Kempf,
402 I., Nykäsenoja, S., Olkkola, S., Wieczorek, K., Amaro, A., Clemente, L., Mossong, J.,
403 Losch, S., Ragimbeau, C., Lund, O., Aarestrup, F.M., 2020. ResFinder 4.0 for
404 predictions of phenotypes from genotypes. *J. Antimicrob. Chemother.* 75, 3491–3500.
405 <https://doi.org/10.1093/jac/dkaa345>.
- 406 7) Buchfink, B., Xie, C., Huson, D.H., 2014. Fast and sensitive protein alignment using
407 DIAMOND. *Nat. Methods* 12, 59–60. <https://doi.org/10.1038/nmeth.3176>
- 408 8) Cacace, D., Fatta-Kassinos, D., Manaia, C.M., Cytryn, E., Kreuzinger, N., Rizzo, L.,
409 Karaolia, P., Schwartz, T., Alexander, J., Merlin, C., Garelick, H., Schmitt, H., de Vries,
410 D., Schwermer, C.U., Meric, S., Ozkal, C.B., Pons, M.N., Kneis, D., Berendonk, T.U.,
411 2019. Antibiotic resistance genes in treated wastewater and in the receiving water
412 bodies: A pan-European survey of urban settings. *Water Res.* 162, 320–330.
413 <https://doi.org/10.1016/j.watres.2019.06.039>
- 414 9) Caucci, S., Karkman, A., Cacace, D., Rybicki, M., Timpel, P., Voolaid, V., Gurke, R.,
415 Virta, M., Berendonk, T.U., 2016. Seasonality of antibiotic prescriptions for outpatients
416 and resistance genes in sewers and wastewater treatment plant outflow. *FEMS*
417 *Microbiol. Ecol.* 92, fiw060. <https://doi.org/10.1093/femsec/fiw060>
- 418 10) Cock, P.J.A., Antao, T., Chang, J.T., Chapman, B.A., Cox, C.J., Dalke, A., Friedberg, I.,
419 Hamelryck, T., Kauff, F., Wilczynski, B., De Hoon, M.J.L., 2009. Biopython: Freely
420 available Python tools for computational molecular biology and bioinformatics.
421 *Bioinformatics* 25, 1422–1423. <https://doi.org/10.1093/bioinformatics/btp163>

- 422 11) Coelho, L.P., Alves, R., Monteiro, P., Huerta-Cepas, J., Freitas, A.T., Bork, P., 2019.
423 NG-meta-profiler: Fast processing of metagenomes using NGLess, a domain-specific
424 language. *Microbiome* 7, 1–10. <https://doi.org/10.1186/s40168-019-0684-8>
- 425 12) Csardi, Gabor, and Tamas Nepusz. 2005. The Igraph Software Package for Complex
426 Network Research. *InterJournal Complex Systems*, 1695
- 427 13) Flynn, T.M., Sanford, R.A., Ryu, H., Bethke, C.M., Levine, A.D., 2013. Functional
428 microbial diversity explains groundwater chemistry in a pristine aquifer Functional
429 microbial diversity explains groundwater chemistry in a pristine aquifer. *BMC Microbiol.*
430 13, 1.
- 431 14) Gatica, J., Jurkevitch, E., Cytryn, E., 2019. Comparative metagenomics and network
432 analyses provide novel insights into the scope and distribution of β -lactamase
433 homologs in the environment. *Front. Microbiol.* 10, 1–11.
434 <https://doi.org/10.3389/fmicb.2019.00146>
- 435 15) Gatica, J., Yang, K., Pagaling, E., Jurkevitch, E., Yan, T., Cytryn, E., 2015. Resistance of
436 undisturbed soil microbiomes to ceftriaxone indicates extended spectrum β -lactamase
437 activity. *Front. Microbiol.* 6, 1–11. <https://doi.org/10.3389/fmicb.2015.01233>
- 438 16) Griebler, C., Avramov, M., 2015. Groundwater ecosystem services : a review 34, 355–
439 367. <https://doi.org/10.1086/679903>.
- 440 17) Griebler, C., Lueders, T., 2009. Microbial biodiversity in groundwater ecosystems.
441 *Freshw. Biol.* 54, 649–677. <https://doi.org/10.1111/j.1365-2427.2008.02013.x>
- 442 18) Hernando-Amado, S., Coque, T.M., Baquero, F., Martínez, J.L., 2019. Defining and
443 combating antibiotic resistance from One Health and Global Health perspectives. *Nat.*
444 *Microbiol.* 4, 1432–1442. <https://doi.org/10.1038/s41564-019-0503-9>

- 445 19) Herrmann, M., Wegner, C.E., Taubert, M., Geesink, P., Lehmann, K., Yan, L., Lehmann,
446 R., Totsche, K.U., Küsel, K., 2019. Predominance of *Cand. Patescibacteria* in
447 groundwater is caused by their preferential mobilization from soils and flourishing
448 under oligotrophic conditions. *Front. Microbiol.* 10, 1–15.
449 <https://doi.org/10.3389/fmicb.2019.01407>
- 450 20) Johnston, S.R., Boddy, L., Weightman, A.J., 2016. Bacteria in decomposing wood and
451 their interactions with wood-decay fungi. *FEMS Microbiol. Ecol.* 92, 1–12.
452 <https://doi.org/10.1093/femsec/fiw179>
- 453 21) Jones, E.R., Van Vliet, M.T.H., Qadir, M., Bierkens, M.F.P., 2021. Country-level and
454 gridded estimates of wastewater production, collection, treatment and reuse. *Earth*
455 *Syst. Sci. Data* 13, 237–254. <https://doi.org/10.5194/essd-13-237-2021>
- 456 22) Kampouris, I.D., Agrawal, S., Orschler, L., Cacace, D., Kunze, S., Berendonk, T.U.,
457 Klümper, U., 2021. Antibiotic resistance gene load and irrigation intensity determine
458 the impact of wastewater irrigation on antimicrobial resistance in the soil microbiome.
459 *Water Res.* 193. <https://doi.org/10.1016/j.watres.2021.116818>
- 460 23) Kampouris, I.D., Alygizakis, N., Klümper, U., Agrawal, S., Lackner, S., Cacace, D.,
461 Kunze, S., Thomaidis, N.S., Slobdonik, J., Berendonk, T.U., 2022. Elevated levels of
462 antibiotic resistance in groundwater during treated wastewater irrigation associated
463 with infiltration and accumulation of antibiotic residues. *J. Hazard. Mater.* 423, 127155.
464 <https://doi.org/10.1016/j.jhazmat.2021.127155>
- 465 24) Karkman, A., Pärnänen, K., Larsson, D.G.J., 2019. Fecal pollution can explain antibiotic
466 resistance gene abundances in anthropogenically impacted environments. *Nat.*
467 *Commun.* 10, 1–8. <https://doi.org/10.1038/s41467-018-07992-3>

- 468 25) Kassambara, A., 2019. ggpubr R Package: ggplot2-Based Publication Ready Plots R
469 package version 0.2.3 <https://CRAN.R-project.org/package=ggpubr>.
- 470 26) Laxminarayan, R., Duse, A., Wattal, C., Zaidi, A.K.M., Wertheim, H.F.L., Sumpradit, N.,
471 Vlieghe, E., Hara, G.L., Gould, I.M., Goossens, H., Greko, C., So, A.D., Bigdeli, M.,
472 Tomson, G., Woodhouse, W., Ombaka, E., Peralta, A.Q., Qamar, F.N., Mir, F., Kariuki,
473 S., Bhutta, Z.A., Coates, A., Bergstrom, R., Wright, G.D., Brown, E.D., Cars, O., 2013.
474 Antibiotic resistance-the need for global solutions. *Lancet Infect. Dis.* 13, 1057–1098.
475 [https://doi.org/10.1016/S1473-3099\(13\)70318-9](https://doi.org/10.1016/S1473-3099(13)70318-9)
- 476 27) Li, H., 2013. Aligning sequence reads, clone sequences and assembly contigs with
477 BWA-MEM 00, 1–3.
- 478 28) Li, H., Durbin, R., 2010. Fast and accurate long-read alignment with Burrows-Wheeler
479 transform. *Bioinformatics* 26, 589–595. <https://doi.org/10.1093/bioinformatics/btp698>
- 480 29) Liao, Z., Chen, Z., Xu, A., Gao, Q., Song, K., Liu, J., Hu, H.Y., 2021. Wastewater
481 treatment and reuse situations and influential factors in major Asian countries. *J.*
482 *Environ. Manage.* 282. <https://doi.org/10.1016/j.jenvman.2021.111976>
- 483 30) Linares, J.F., Gustafsson, I., Baquero, F., Martinez, J.L., 2006. Antibiotics as
484 intermicrobiol signaling agents instead of weapons. *Proc. Natl. Acad. Sci. U. S. A.* 103,
485 19484–19489. <https://doi.org/10.1073/pnas.0608949103>
- 486 31) Martin, M. 2011. Cutadapt removes adapter sequences from high-throughput
487 sequencing reads. *EMBnet.journal*, 17(1), pp. 10-12.
488 doi:<https://doi.org/10.14806/ej.17.1.200>
- 489 32) Miao, V, Davies, J. Actinobacteria: The good, the bad, and the ugly. *Antonie van*
490 *Leeuwenhoek, Int J Gen Mol Microbiol* 2010; 98: 143–150.

- 491 33) Nawaz, A., Purahong, W., Lehmann, R., Herrmann, M., Totsche, K.U., Küsel, K., Wubet,
492 T., Buscot, F., 2018. First insights into the living groundwater mycobiome of the
493 terrestrial biogeosphere. *Water Res.* 145, 50–61.
494 <https://doi.org/10.1016/j.watres.2018.07.067>
- 495 34) Nesme J, Simonet P. The soil resistome: A critical review on antibiotic resistance origins,
496 ecology and dissemination potential in telluric bacteria. *Environ Microbiol* 2015; 17:
497 913–930.
- 498 35) Oksanen; J., Blanchet; F.G., Friendly; M., Kindt; R., Legendre; P., McGlinn; D., Minchin;
499 P.R., O'Hara; R.B., Simpson; G.L., Solymos; P.M. Stevens; H.H., Szoecs; E., Wagner
500 H., 2019. *vegan* R package: an R package for community ecologists. R package
501 version 2.5-6. <https://cran.rproject.org/package=vegan>
- 502 36) Pedersen T (2022). *ggraph*: An Implementation of Grammar of Graphics for Graphs and
503 Networks. <https://ggraph.data-imaginist.com>, <https://github.com/thomasp85/ggraph>.
- 504 37) R Core Team, R: A language and environment for statistical computing R Foundation for
505 Statistical Computing, Vienna, Austria (2019)
- 506 38) Retter, A., Karwautz, C., Griebler, C., 2021. Groundwater microbial communities in times
507 of climate change. *Curr. Issues Mol. Biol.* 41, 509–538.
508 <https://doi.org/10.21775/cimb.041.509>
- 509 39) Sonthiphand, P., Ruangroengkulrith, S., Mhuantong, W., Charoensawan, V.,
510 Chotpantararat, S., Boonkaewwan, S., 2019. Metagenomic insights into microbial
511 diversity in a groundwater basin impacted by a variety of anthropogenic activities.
512 *Environ. Sci. Pollut. Res.* 26, 26765–26781. [https://doi.org/10.1007/s11356-019-](https://doi.org/10.1007/s11356-019-05905-5)
513 [05905-5](https://doi.org/10.1007/s11356-019-05905-5)

- 514 40) Spielmeier A, Höper H, Hamscher G. Long-term monitoring of sulfonamide leaching
515 from manure amended soil into groundwater. *Chemosphere* 2017; 177: 232–238.
- 516 41) Szekeres, E., Chiriac, C.M., Baricz, A., Szőke-Nagy, T., Lung, I., Soran, M.L., Rudi, K.,
517 Dragos, N., Coman, C., 2018. Investigating antibiotics, antibiotic resistance genes, and
518 microbial contaminants in groundwater in relation to the proximity of urban areas.
519 *Environ. Pollut.* 236, 734–744. <https://doi.org/10.1016/j.envpol.2018.01.107>
- 520 42) Taş, N., Brandt, B.W., Braster, M., van Breukelen, B.M., Röling, W.F.M., 2018.
521 Subsurface landfill leachate contamination affects microbial metabolic potential and
522 gene expression in the Banisveld aquifer. *FEMS Microbiol. Ecol.* 94, 1–12.
523 <https://doi.org/10.1093/femsec/fiy156>
- 524 43) Vaz-Moreira, I., Nunes, O.C., Manaia, C.M., 2014. Bacterial diversity and antibiotic
525 resistance in water habitats: Searching the links with the human microbiome. *FEMS*
526 *Microbiol. Rev.* 38, 761–778. <https://doi.org/10.1111/1574-6976.12062>
- 527 44) Wang, H., Su, X., Su, J., Zhu, Y., Ding, K., 2022. Profiling the antibiotic resistome in soils
528 between pristine and human-affected sites on the Tibetan Plateau. *J. Environ. Sci.*
529 (China) 111, 442–451. <https://doi.org/10.1016/j.jes.2021.04.019>
- 530 45) Wickham H. *ggplot2: Elegant Graphics for Data Analysis*. Springer (2016)
- 531 46) Wickham, H., François, R., Henry, L., Müller, K. 2022. *dplyr: A Grammar of Data*
532 *Manipulation*. <https://dplyr.tidyverse.org>, <https://github.com/tidyverse/dplyr>.
- 533 47) Wickham; H., Averick; M., Bryan; J., Chang; W., McGowan; L., François; R., Golemund;
534 G., Hayes; A., Henry; L., Hester; J., Kuhn; M., Pedersen; T., Miller; E., Bache; S.,
535 Müller; K., Ooms; J., Robinson; D., Seidel; D., Spinu; V., Takahashi; K., Vaughan; D.,

- 536 Wilke; C., Woo; K., Yutani; H. Welcome to the Tidyverse. J. Open Source Softw. 2019;
537 4 (43); 1686. <https://doi.org/10.21105/joss.01686>.
- 538 48) Yan L, Herrmann M, Kampe B, Lehmann R, Totsche KU, Küsel K. Environmental
539 selection shapes the formation of near-surface groundwater microbiomes. Water Res
540 2020; 170: 115341.
- 541 49) Zaouri, N., Jumat, M.R., Cheema, T., Hong, P.Y., 2020. Metagenomics-based evaluation
542 of groundwater microbial profiles in response to treated wastewater discharge.
543 Environ. Res. 180, 108835. <https://doi.org/10.1016/j.envres.2019.108835>
- 544 50) Zhang, Y. Zhang, Yuanzhu, Kuang, Z., Xu, J., Li, C., Li, Y., Jiang, Y., Xie, J., 2019.
545 Comparison of Microbiomes and Resistomes in Two Karst Groundwater Sites in
546 Chongqing, China. Groundwater 57, 807–818. <https://doi.org/10.1111/gwat.12924>